World Academy of Science, Engineering and Technology
International Journal of Electronics and Communication Engineering
Vol:2, No:5, 2008

Improvement of Synchronous Machine Dynamic Characteristics via Neural Network Based Controllers

S. A. Gawish, F. A. Khalifa, and R. M. Mostafa

Open Science Index, Electronics and Communication Engineering Vol:2, No:5, 2008 publications.waset.org/985/pdf

***Abstract*—**This paper presents Simulation and experimental study aimed at investigating the effectiveness of an adaptive artificial neural network stabilizer on enhancing the damping torque of a synchronous generator. For this purpose, a power system comprising a synchronous generator feeding a large power system through a short tie line is considered. The proposed adaptive neuro-control system consists of two multi-layered feed forward neural networks, which work as a plant model identifier and a controller. It generates supplementary control signals to be utilized by conventional controllers. The details of the interfacing circuits, sensors and transducers, which have been designed and built for use in tests, are presented. The synchronous generator is tested to investigate the effect of tuning a Power System Stabilizer (PSS) on its dynamic stability. The obtained simulation and experimental results verify the basic theoretical concepts.

***Keywords*—**Adaptive artificial neural network, power system stabilizer, synchronous generator.

I. Introduction

THE first step in a stability study or a dynamic behavior investigation is to develop a mathematical model of the system under study during transient conditions. The main focus on such a model is on those elements affecting the acceleration (or deceleration) of the machine rotors. The complexity of the Model depends upon the type of the transients and the system to be investigated. Generally, the components of the power system that influence the electromechanical torque of the machines should be included in the model.

A three-phase generator is connected to a network through a transformer and transmission line as shown in Fig. 1. The generator is connected to an excitation system and driven by a hydraulic turbine and governor.

S. A. Gawish is with Former Head of Electrical Power and Energy Dept., Military Technical College, Cairo, Egypt.

F. A. Khalifa is with Vice President of Suez Canal University, Suez Branch, Egypt.

R. M. Mostafa is with Dean of Faculty of Industrial Education, Beni Suief University, Egypt.

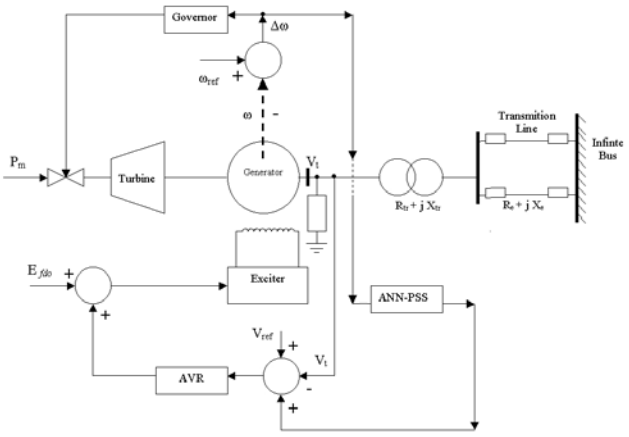


Fig. 1 System under study

II. Mathematical Model of the System Under Study

The mathematical model of the power system under study here is based on the state space approach [1]. The power system is described by the differential equations representing its components which can be solved on a digital computer using a numerical integration technique. The computer program of the power system model is designed such that both transient and dynamic response of the generator to different types of disturbances can be computed. The large system bus voltage and frequency are assumed to be constant at their rated values. The transmission line is represented by its lumped resistance and inductance model.

One of the systematic ways of obtaining the state space form is described in the following:

$$[V] = [L][i^{\bullet}] + [D][i] \tag{1}$$

Where:

$$[V] = \begin{bmatrix} v_d \\ v_q \\ v_{fd} \\ 0 \\ 0 \end{bmatrix} ; \quad [L] = \begin{bmatrix} -X_d & 0 & X_{ad} & X_{ad} & 0 \\ 0 & -X_q & 0 & 0 & X_{aq} \\ -X_{ad} & 0 & X_{ffd} & X_{ad} & 0 \\ -X_{ad} & 0 & X_{ad} & X_{kkd} & 0 \\ 0 & -X_{aq} & 0 & 0 & X_{kkq} \end{bmatrix}$$

$$[D]=\begin{bmatrix} -(r+\mathrm{R_e}) & \omega(X_q+X_e) & 0 & 0 & -\omega X_{aq} \\ -\omega(X_d+X_e) & -(r+\mathrm{R_e}) & \omega X_{ad} & \omega X_{ad} & 0 \\ 0 & 0 & r_{fd} & 0 & 0 \\ 0 & 0 & 0 & r_{kd} & 0 \\ 0 & 0 & 0 & 0 & r_{kq} \end{bmatrix}$$

The stator self-reactances X_d, X_q are modified by adding the tie-line reactance X_e to each of them. Also, the stator phase resistance should be modified by adding the tie-line resistance to it.

The state space form of the voltage equation can then be obtained as:

$$[i]^{\bullet} = -[L]^{-1}[D][i] + [L]^{-1}[V]$$

Which can be written in the well - known state space form

$$[i]^{\bullet} = [A][i] + [B][V] \tag{2}$$

Where: $[A] = -[L]^{-1}[D]$ and $[B] = [L^{-1}]$

The swing equations can be split into two first order equations as follows.

$$\omega^{\bullet} = \frac{T_i - T_{em}}{H'} \tag{3}$$

$$\delta^{\bullet} = \omega - \omega_{ref} \tag{4}$$

Where $T_{em} = i_q \psi_d - i_d \psi_q$ (5)

$$T_{em} = i_q\ [-i_d L_d + i_{fd} L_{ad} + i_{kd} L_{ad}] - i_d[-L_q i_q + L_{aq} i_{kq}] \tag{6}$$

This equation is a nonlinear equation. The final form of the state space model is given by equation (7)

$$\begin{pmatrix} i_d^{\bullet} \\ i_q^{\bullet} \\ i_{fd}^{\bullet} \\ i_{kd}^{\bullet} \\ i_{kq}^{\bullet} \\ \omega^{\bullet} \\ \delta^{\bullet} \end{pmatrix} = \begin{pmatrix} & \mathbf{A} & & & & & 0 & 0 \\ & & & & & & 0 & 0 \\ & & & & & & 0 & 0 \\ & & & & & & 0 & 0 \\ & & & & & & 0 & 0 \\ \dots & \dots & \dots & \dots & \dots & \dots & \dots & \dots \\ \frac{X_d i_{q0}}{(H)} & \frac{-X_q i_{d0}}{(H)} & \frac{-X_{ad} i_{q0}}{(H)} & \frac{-X_{ad} i_{q0}}{(H)} & \frac{X_{aq} i_{d0}}{(H)} & & 0 & 0 \\ 0 & 0 & 0 & 0 & 0 & & 1 & 0 \end{pmatrix} \begin{pmatrix} i_d \\ i_q \\ i_{fd} \\ i_{kd} \\ i_{kq} \\ \omega \\ \delta \end{pmatrix}$$

$$+ \begin{pmatrix} & \mathbf{B} & & & & & 0 & 0 \\ & & & & & & 0 & 0 \\ & & & & & & 0 & 0 \\ & & & & & & 0 & 0 \\ & & & & & & 0 & 0 \\ \dots & \dots & \dots & \dots & \dots & \dots & \dots & \dots \\ 0 & 0 & 0 & 0 & 0 & \frac{1}{H} & 0 & \\ 0 & 0 & 0 & 0 & 0 & 0 & -1 & \end{pmatrix} \begin{pmatrix} v_d \\ v_q \\ v_{fd} \\ 0 \\ 0 \\ T_i \\ \omega_{ref} \end{pmatrix}$$

The speed governing system will be represented by a nonlinear hydraulic turbine model, a PID (Proportional plus Integral plus Derivative) governor system, and a servo-motor [2].

The Excitation System block is a simplified model derived from the IEEE standards [3]. The basic elements that form the excitation system block are the voltage regulator and the exciterwhere:

$$\frac{E_{fd}}{V_R} = \frac{1}{K_e + s\,T_e} \tag{8}$$

The excitation system, described by the block diagram of Fig. 2, is used to represent field controlled dc exciter with continuously acting voltage regulators.

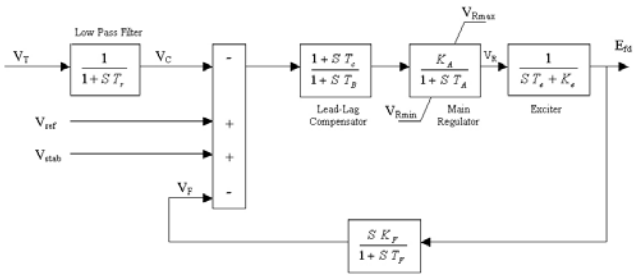


Fig. 2 Block diagram for the AVR and exciter model

The complete model of the power system under consideration is obtained by adding the differential equations describing the performance of the excitation system, speed governor, and the differential equations describing the generator operation together with the transmission system, which consists of a transformer and a transmission line. Due to the characteristics of Artificial Neural Networks (ANN), they have been applied to deal with the stability problem of synchronous generators [5-9].

III. Modeling of the ANN Controller

The model reference control architecture used is shown in Fig. 3. The design process for the proposed controller is divided into two steps, as two neural networks will be constructed.

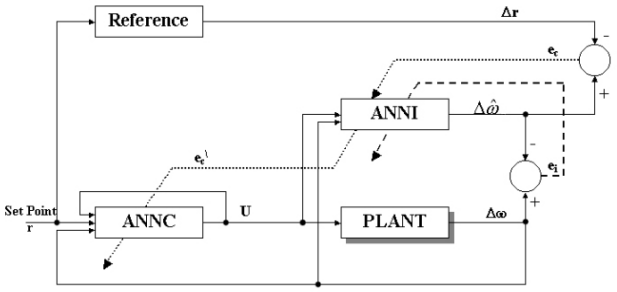


Fig. 3 ANN-PSS architecture

The ANN identifier (ANNI) architecture as shown in Fig. 4, consists of three layers and has two inputs and one output.

Open Science Index, Electronics and Communication Engineering Vol:2, No:5, 2008 publications.waset.org/985/pdf

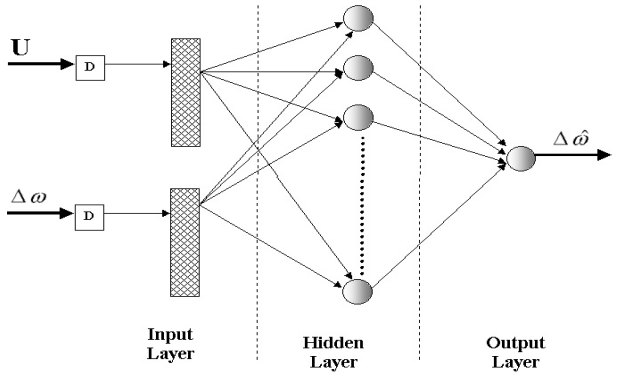


Fig. 4 Hierarchical architecture ANNI

The ANN controller (ANNC) architecture, as shown in Fig. 5 consists of three layers and has three inputs and one output

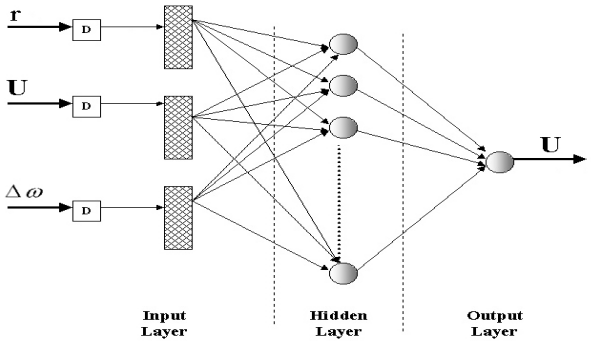


Fig. 5 Hierarchical architecture ANNC

A. Plant Model Back Propagation Algorithm

The input vector to the plant model is:

[V_f (K-1), V_f (k-2)… V_f (k-m), ω (K-1), ω (K-2)… ω (K-n)]

Where V_f (K-1) and ω (K-1) is delayed controller output and the delayed plant output respectively. The cost function used for the plant model is:

$$J_i(K) = \frac{1}{2} e_i(K)^2 = \frac{1}{2}[\omega(K-1) - \omega(K)]^2 \quad (9)$$

The weights are updated as:

$$W_i(K) = W_i(K-1) - \eta_i \nabla W_i J_i(K) \quad (10)$$

In which W_i (K) is the matrix of identifier weights of time step K and η_i is the learning rate for the plant model. The gradient $\nabla W_i J_i$ (K) is computed by:

$$\nabla W_i J_i(K) = -[W_i(K-1) - W_i(K)] \frac{\partial W(K)}{\partial W_i(K)} \quad (11)$$

From equations (10) and (11), the cost function J_i (K) is minimized in each sampling period by the back-propagation cycle to the scalar error.

$[\omega(K-1) - \omega(K)]$

B. Adaptive Neuro-Controller Backpropagation Algorithm

The input vector to the neuro-controller is

[ωr (K-1), ωr (K-2)… ωr (K-P), Vf (K-1), Vf (K-2)… Vf (k-m), ω (K-1), ω (K-2)… ω (K-n)] (12)

Where ωr (K-1), Vf (K-1) and ω (K-1) are the delayed reference input, delayed controller output and the delayed plant output, respectively [10].

The cost function for the controller is considered as:

$$J_C(K) = \frac{1}{2}[e_c(K)^2 + h\,u(K)^2] = \frac{1}{2}[\omega_d(K) - \omega(K)]^2 + \frac{h}{2}u(K)^2 \quad (13)$$

Where W_d (K) is the desired speed deviation at time step K that is equal to zero in a regulatory setup. And h is a tuning parameter, which is used to improve the plant output dynamic characteristics. By taking h greater than zero, a penalty factor is applied to the control action generated by the Adaptive Artificial Neural PSS, which helps the tuning of the dynamic trajectory and optimizing the overshoot and settling time of the response curve.

The weights of the controller, W_c (K), are updated as:

$$W_C(K) = W_C(K-1) - \eta_C \nabla W_C J_C(K) \quad (14)$$

Where η_c is the controller-learning rate and the gradient $\nabla W_c J_c$ (K) is defined as:

$$\nabla W_C J_C(K) = \left[W(K) \frac{\partial W(K)}{\partial u(K)} + h\,u(K) \right] \frac{\partial u(K)}{\partial W_C(K)} \quad (15)$$

By using equations (14) and (15), J_c (K) is minimized in each sampling period by the back-propagation cycle to the scalar error $[\omega(K-1) - \omega(K)]$.

IV. Experimental Setup

The experimental set-up shown in Figs. 6, 7 is constructed and tested .The hardware components are composed of:

Three phase supply – DC shunt motor – Control unit for the motor – Synchronous Machine – Excitation voltage controller – Tacho generator – Couplings – Resistive, inductive and capacitive loads – Transmission lines Circuit breaker – Voltage transducer – Microcomputer – and different measuring units.

The synchronous machine is driven by the dc shunt motor and it is connected to an infinite bus through two transmission lines. The generator terminal voltage is monitored by the microcomputer through a voltage transducer and data acquisition card. The feedback from the microcomputer is connected to the excitation control unit, leading to an increase or decrease in the excitation voltage of the generator. The speed of the machine is converted to volt by means of a tacho generator, which is fed to the microcomputer through the data acquisition card. All signals coming from the data acquisition card are supplied to the MATLAB using the Real Time Toolbox. All comparisons and control decisions are taken in the MATLAB environment and the feedback action is applied to the system through the data acquisition card.

As shown in Fig. 8, the signal from the Tacho generator is supplied to the microcomputer through input channel 1 and is compared with the reference speed signal. The difference between these two signals indicates the change in the speed (Δ ω), which is applied to the power system stabilizer (PSS). The

Open Science Index, Electronics and Communication Engineering Vol:2, No:5, 2008 publications.waset.org/985/pdf

output signals from the voltage transducers are supplied to the microcomputer through input channel 2, which is compared with the reference signal. The difference between these two signals indicates the change in the generator terminal voltage. The output from the PSS is added to the change in the generator terminal voltage to give the total error signal (V_e). According to V_e value, the decision of increasing or decreasing the excitation voltage of the generator is taken.

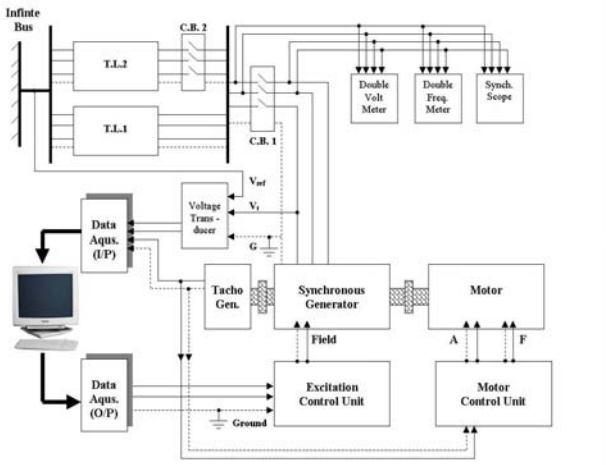


Fig. 6 The experimental setup

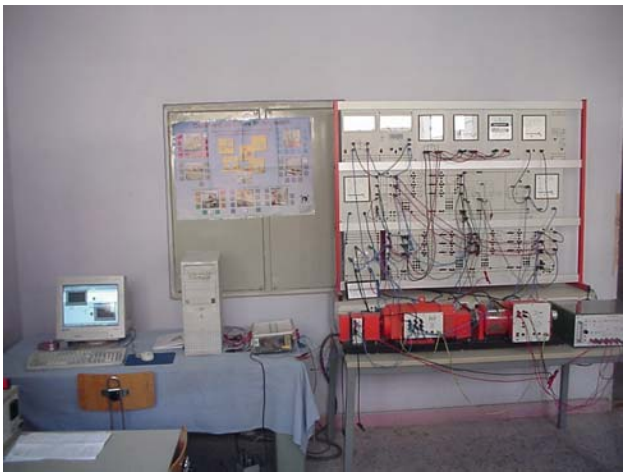


Fig. 7 General view of the complete experiment

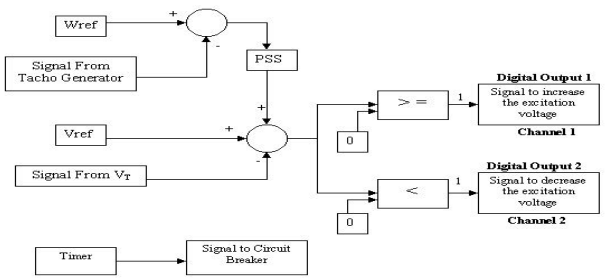


Fig. 8 Schematic diagram for the control strategy

V. Simulation and Experimental Results

A. Without the Proposed ANN-PSS

The Conventional PSS (CPSS) used in this paper, as shown in Fig. 9, is a proportional - integral - derivative power system stabilizer (PID-PSS). It is designed and implemented in the system, firstly to generate training data for the proposed ANN-PSS by fine tuning of its gains under different operating points and secondly, to be a base for comparison with the ANN-PSS under different operating points and different disturbances. In this case its gain is kept fixed for all operating points. The system response when provided with such a CPSS is shown in Figs. 10-15 for the case of a sudden disconnection of one of the two parallel transmission lines followed by the reconnection of the disconnected line. The system is initially loaded by P = 0.75 p.u. and Q = 0.3 (p.u.) (Inductive).Investigation of Figs. 10-15, shows that, the agreement between the simulation and experimental results can be seen.

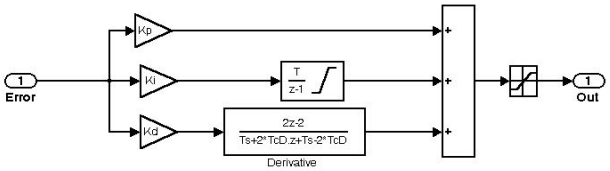


Fig. 9 The PID-PSS structure

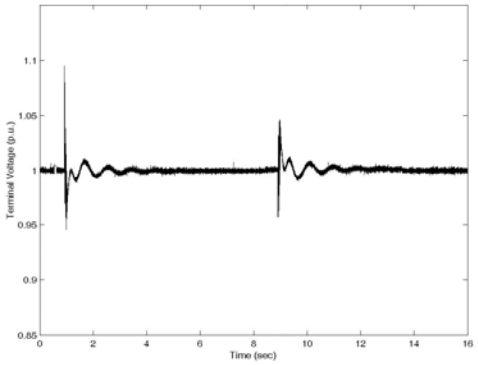


Fig. 10 Terminal voltage variation following the disconnection of one of the two T.L. with CPSS at P = 0.75 pu and Q = 0.3 pu (Simulation)

Open Science Index, Electronics and Communication Engineering Vol:2, No:5, 2008 publications.waset.org/985/pdf

Open Science Index, Electronics and Communication Engineering Vol:2, No:5, 2008 publications.waset.org/985/pdf

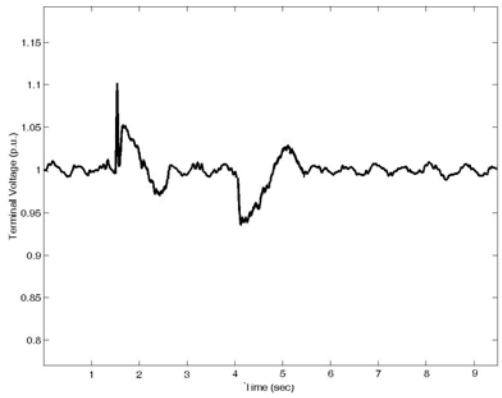


Fig. 11 Terminal voltage variation following the disconnection of one of the two T.L. with CPSS at P = 0.75 pu and Q = 0.3 pu (Experimental)

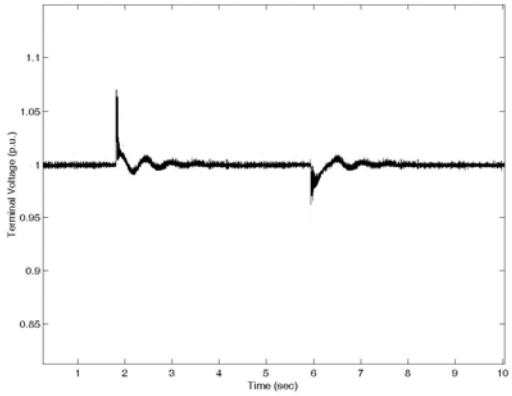


Fig. 12 Terminal voltage variation following the disconnection of one of the two T.L. with CPSS at P = 0.55 pu and Q = 0.3 pu (Simulation)

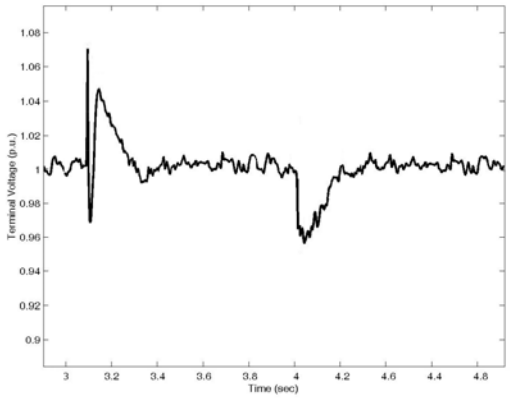


Fig. 13 Terminal voltage variation following the disconnection of one of the two T.L. with CPSS at P = 0.55 pu and Q = 0.3 pu (Experimental)

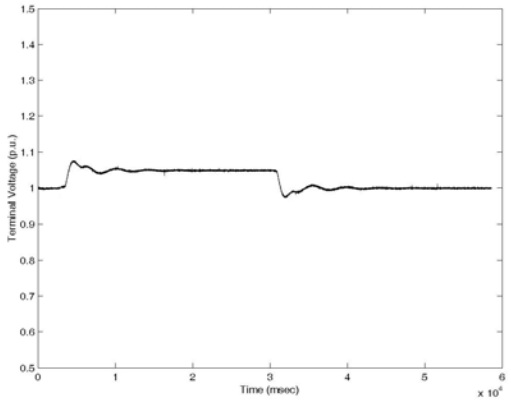


Fig. 14 Terminal voltage variation following the 5 % step increase in Vref with CPSS at P = 0.75 pu and Q = 0.3 pu (Simulation)

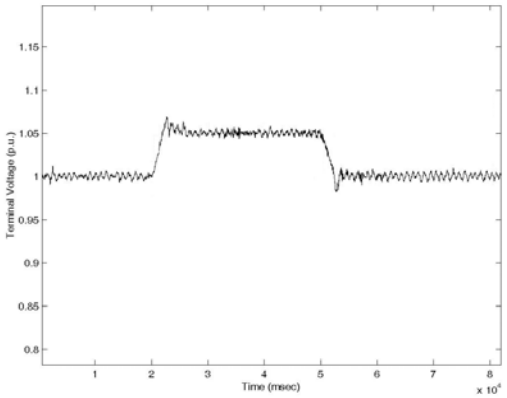


Fig. 15 Terminal voltage variation following the 5 % step increase in Vref with CPSS at P = 0.75 pu and Q = 0.3 pu (Experimental)

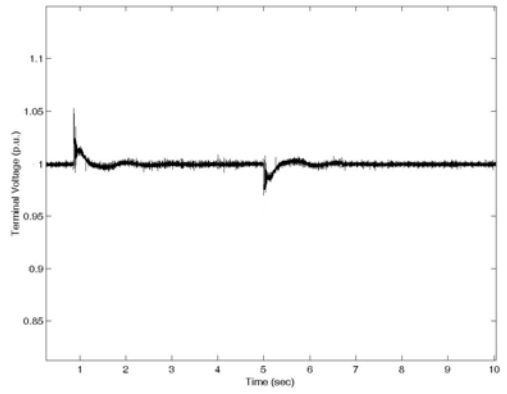


Fig. 16 Terminal voltage variation following the disconnection of one of the two T.L. with ANN-PSS at P = 0.55 pu and Q = 0.3 pu (Simulation)

Open Science Index, Electronics and Communication Engineering Vol:2, No:5, 2008 publications.waset.org/985/pdf

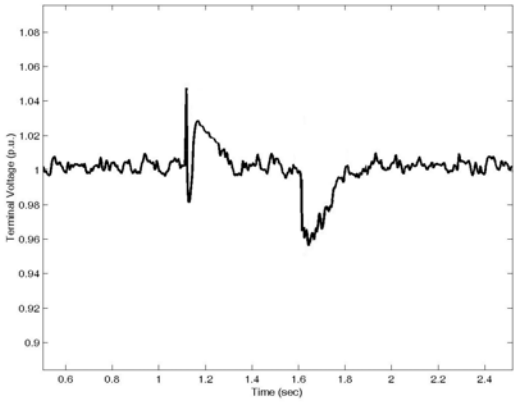


Fig. 17 Terminal voltage variation following the disconnection of one of the two T.L. with ANN-PSS at P = 0.55 pu and Q = 0.3 pu (Experimental)

B. With the Proposed ANN-PSS

The performance of the proposed ANN-PSS has been investigated through a number of tests for a variety of operating conditions and disturbances. Some of these results are presented in this section. The results are compared with the same system when controlled by a CPSS, tuned at P = 0.75 p.u. Q = 0.3 p.u. The transient response of the power system under study, under different operating conditions, and types of disturbances, represented in the change in terminal voltage (p.u.) has been obtained and presented in Figs. 16-23.

The obtained results show the superiority of the proposed ANN – PSS when compared with the conventional PSS, at the same operating conditions. Investigation of the experimental results verifies the effectiveness of the professed PSS in enhancing the damaging performance of the system under consideration.

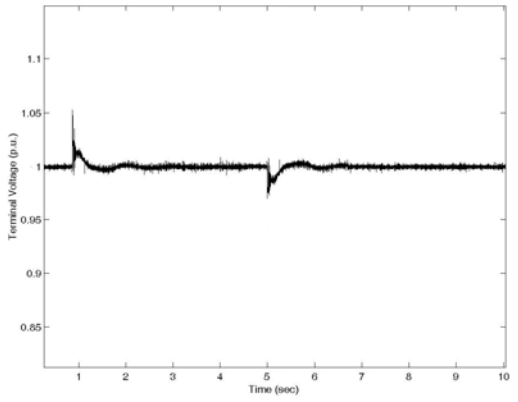


Fig. 18 Terminal voltage variation following the disconnection of one of the two T.L. with ANN-PSS at P = 0.75 pu and Q = 0.3 pu (Simulation)

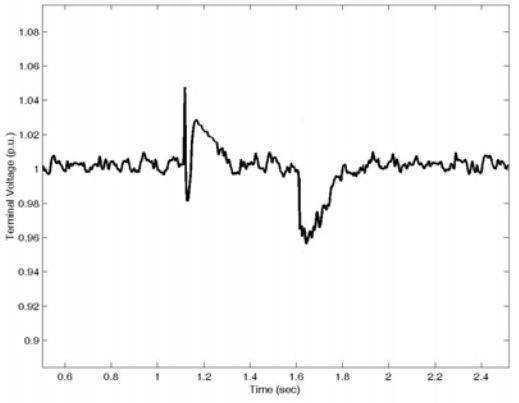


Fig. 19 Terminal voltage variation following the disconnection of one of the two T.L. with ANN-PSS at P = 0.75 pu and Q = 0.3 pu (Experimental)

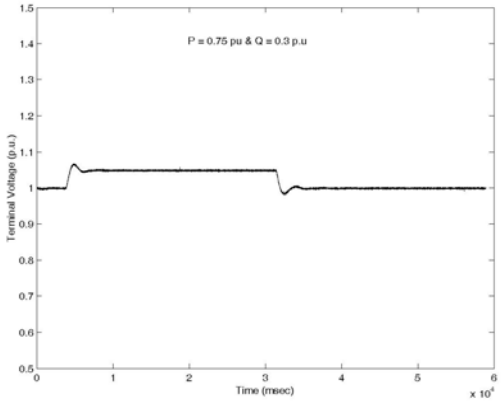


Fig. 20 Terminal voltage variation following the 5 % step increase in Vref with ANN-PSS at P = 0.75 pu and Q = 0.3 pu (Simulation)

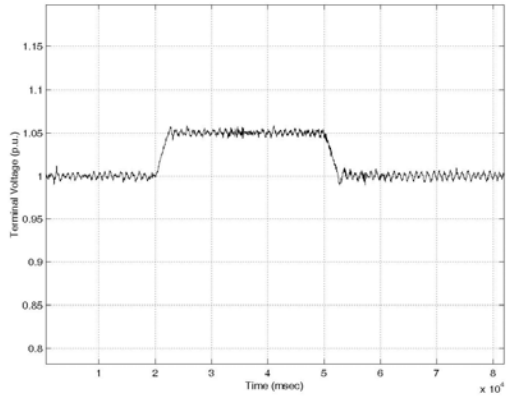


Fig. 21 Terminal voltage variation following the 5 % step increase in Vref with ANN-PSS at P = 0.75 pu and Q = 0.3 pu (Experimental)

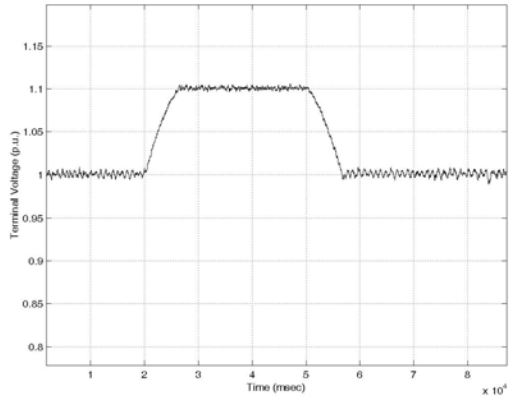


Fig. 22 Terminal voltage variation following the 10 % step increase in Vref with ANN-PSS at P = 0.75 pu and Q = 0.3 pu (Experimental)

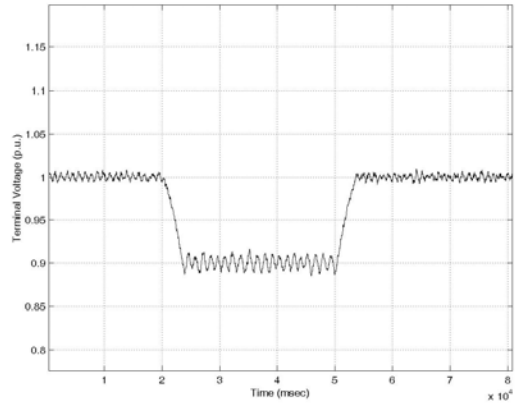


Fig. 23 Terminal voltage variation following the 10 % step decrease in V_{ref} with ANN-PSS at P = 0.75 pu and Q = 0.3 pu (Experimental)

VI. CONCLUSION

The prosed power system stabilizer is found to enjoy far superior performance when compared with conventional power system stabilizers. As a result, the proposed controller can work efficiently with systems characterized by a wide range os system operation conditions.

This paper presents in addition experimental work aimed at verifying the baseic concepts presented in the thesis. For this purpose, an experimental setup has been implemented. This comprises the different electronic transducers, three phasesupply, DC shunt motor, contorl unit for the motor, synchronous machine, excitation voltage controller, Tacho generator, couplings, resistive, inductive and copaciitivel loads, transmission lines, circuit breaker, microcomputer, and different measuring units.

The implemented system is tested through the application of different types of disturbances. The obtained tranient response is then examined and compared with that obtained from the digital simulation study. The agreement of both groups of characteristics confirms the validity of the work presented in this paper.

REFERENCES

[1] Anderson P. M. and Fouad A. A., ' Power System Control Stability", Vol.1, The Iowa State University press, 1977.
[2] IEEE Working Group on Prime Mover and Energy Supply Models for System Dynamic Performance Studies. "Hydraulic Turbine and Yurbine Control Models for Dynamic Studies". IEEE Trans. On Power Systems, Vol. 7, No. 1, Fep.1992, PP.167-179
[3] "Recommended Practice for Excitation System Modeles for Power System Stability Studies ". IEEE Standards 421.5-1992, August 1992.
[4] Hassan Bevarni, Takashi hiyama and yasunori mitani," Power System Dynamic Stability and voltage Regulation Enhancement Using an Optimal Gain Vector." Control Engineering Practice, Jan., 2008. Available at WWW. Science direct. Com
[5] Y Zhang, G. P. Chen, O. P. Malik and G. S. Hope, "An Artificial Neural Network Based Power System Stabilizer ", IEEE Trans. On Energy Conv., Vol.8, No.1, PP 71-77, March 1993.
[6] Shiji Cheng, Rujing Zhou and Lin Guan, "An on – line self-Learning Power System Stabilizer using a neural network method", IEEE Trans. Power System. Vol. 12, No.2, May 1997.
[7] S. Chusanapiputt and K. Withirom present," Parameter tuning of the conventional power system stabilizer by Artificial Neural Network.", Conf.on Power System Technology, 2004, Bangkok, Thailand.
[8] Wenxin liu and Ganesh K. Venayagamorthy," Design of an Adaptive neural network Based power system stabilizer." Neural networks, Vol.16, June – July 2003, p.p.891-898.
[9] Jesus Fraile – Ardanvy, P.J. Zufiria," Design and comparison of Adaptive Power system stabilizers Based on Neural Fuzzy Networks and Genetic Algorithms." Neurocomputing, Vol.70, Oct.2007 pp. 2902-2912.
[10] P. Shamsollahi and O.P. Malik, "Design of a Neural Adaptive power system Using Dynamic Back – Propagation Method.", Int. Journal of Elect. Power & Energy systems, Vol.22, Jan. 2000 PP.29-34.

Open Science Index, Electronics and Communication Engineering Vol:2, No:5, 2008 publications.waset.org/985/pdf